Numerical Simulation of Mass Transfer Performance of Sieve Distillation Trays

X. Y. You

School of Environmental Science and Engineering, Tianjin University,
300072, Tianjin, P.R. China

A turbulent mixed two-phase flow model is employed to predict the flow on a column distillation tray by considering the resistance and the enhanced turbulence, which are created by the uprising vapor. The tray flow patterns of our numerical model are confirmed satisfactorily by the experimental measurements. The dependence of mass transfer performance of sieve distillation tray on the physical properties of fluid and tray flow patterns is quantitatively analyzed. Furthermore, the ways to improve the efficiency of distillation sieve are discussed.

Keywords:
Turbulent two-phase flow, mass transfer performance, distillation, CFD

Introduction

Distillation is a widely used method to separate liquid mixtures into their components and has been applied in many separation processes such as those in petroleum, petrochemical, chemical and related industries. It shares a large portion of the capital investment, and is the largest consumer of energy in those industries. It is also commonly recognized that distillation is a very important process in today's industry and will continue to be in the future.

Even if the distillation is very old in art, its design method is still lacking a sound basis. For example, although it is well known that the liquid flow pattern, or velocity distribution, is a very important factor in distillation tray design, its evaluation has long been relied mainly on designer's experience or experiment, implicitly in the estimation of tray effectiveness. With the rapid development of computational fluid dynamics (CFD), more reliable theoretical approach of such problem is possible. The tray design based on such scientific foundation is obviously superior to that based on experience or rough estimation, especially for the case of scaling up a column to large diameter.

The complication of liquid flow pattern on a column tray comes from the fact that, liquid flowing is aerated through a curved convergent-divergent open channel with structural resistance and subject simultaneously to the action of the cross current uprising vapor. Based on two-dimensional flow with some simplifying assumptions, *Yoshida*[1] presented a direct numerical solution for Navier-Stokes equations in stream function form, nevertheless his result has not been confirmed by experiment. *Zhang* and *Yu*[2], *Yu* et al.[3] and *Liu* et al.[4] formulated a single-fluid (liquid) model and *Yuan* et al.[5] and *Yu* et al.[6] formulated a two-fluid (liquid and vapor) model for describing the flow patterns on tray. In all these studies, the $K - \varepsilon$ model is employed to close the Reynolds stress. Their predictions of liquid velocity distribution on the tray were satisfactorily confirmed by the experimental results. The two-fluid model gives slightly better results than those of single-fluid model at the expense of much more complicated computation. *Krishna* et al.[7] and *Baten* and *Krishna*[8] presented a three-dimensional CFD model and computed by using CFX software for simulating flow field on sieve tray. They found strong 3D effects at the inlet and outlet of a tray and insisted that the 3D simulation is required to include the variations of liquid flow pattern in vertical dimension. However, their test column is of very small diameter, i.e. a very short liquid path in combination with a rather large weir height. From our experimental work and three-dimensional calculation by using commercial software, the steady flow pattern on a tray is mainly two-dimensional except in the regions near the inlet and the outlet weirs and in the thin layer close to the tray floor. We expect that these three-dimensional effects on the flow distribution may be diminished, in percentage of total flow, with the increase of column diameter. Thus, we assume that such three-dimensional effects are negligible here and a two-dimensional flow model can be applied to simulate the flow distribution on the tray.

Yu et al.[3] studied the concentration field on a sieve tray by applying the CFD method to solve the flow and mass transfer equations with the assumption of constant equilibrium ratio of the separated substance in the mixture. They obtained the mass transfer efficiency in terms of effectiveness of the

tray. But their assumption of constant equilibrium ratio would lead to a large deviation in the case of having wide range of tray concentration. Therefore, a variable equilibrium ratio is adopted to recalculate the concentration field on the tray in this study. Furthermore, the dependence of mass transfer efficiency of sieve distillation tray on the physical properties of fluid and tray flow patterns is quantitatively analyzed and the ways to improve the efficiency of sieve distillation are discussed.

Theoretical model

Two-phase flow model

In this paper, we present a two-phase flow model consisting of a continuous liquid phase and a vapor phase dispersed in the form of bubbles and/or froth in the (continuous) liquid phase. The basic equations derived by *Elghobashi* and *Abou-Arab*[9] for laminar two-phase flows are adopted here. The steady volume average mass and momentum equations for liquid phase are

$$(\rho_1 \phi_1 U_i)_{;i} = 0, \tag{1}$$

$$(\rho_1 \phi_1 U_j U_i)_{;j} = -(1 - M\phi_2)p_{;i} - ME\phi_2(U_i - V_i)$$
$$+ [\mu_1 \phi_1 (U_{i;j} + U_{j;i})]_{;j} - \frac{2}{3}(\mu_1 \phi_1 U_{l;l})_{;i} + f_1. \tag{2}$$

The corresponding equations for vapor phase, i.e. carrying bubbles and froth are

$$(\rho_2 \phi_2 V_i)_{;i} = 0, \tag{3}$$

$$(\rho_2 \phi_2 V_j V_i)_{;j} = -\phi_2 p_{;i} + E\phi_2(U_i - V_i)$$
$$+ [\mu_2 \phi_2 (V_{i;j} + V_{j;i})]_{;j} - \frac{2}{3}(\mu_2 \phi_2 V_{l;l})_{;i} + f_2. \tag{4}$$

and the global continuity equation is

$$\phi_1 + \phi_2 = 1. \tag{5}$$

In equations (1)-(4), the partial derivatives are represented by a subscript consisting a semicolon and an index [e.g., $U_{i;j} = \partial U_i / \partial x_j$, $U_{i;jl} = \partial^2 U_i / \partial x_j \partial x_l$]. M is the local effectiveness of momentum transfer from the dispersed phase to the continuous phase. $M = 1$ is chosen here by assuming a perfect momentum exchange between the two phases.

Assuming that, in the flowing aerated liquid, the velocity of carrying bubbles and froth V_i is equal to that of liquid phase U_i. By adding equations (1) and (3), simplifying the result and applying equation (5), we have

$$(\rho U_i)_{;i} = 0. \tag{6}$$

Similarly by adding equations (2) and (4), it results

$$(\rho U_j U_i)_{;j} = -p_{;i} + [\mu(U_{i;j} + U_{j;i})]_{;j} -$$
$$- \frac{2}{3}(\mu U_{l;l})_{;i} + f. \tag{7}$$

where $\rho = \rho_1 \phi_1 + \rho_2 \phi_2$ and $\mu = \mu_1 \phi_1 + \mu_2 \phi_2$ are the density and viscosity of mixture.

For turbulent flow, the volume fractions ϕ_1 and ϕ_2 are separated as a mean value and a disturbance

$$\phi_1 = \bar{\phi}_1 + \phi_1', \quad \phi_2 = \bar{\phi}_2 + \phi_2'. \tag{8}$$

The above equations lead to a flow with variable density and viscosity even if the density and viscosity of the two phases are assumed to be constants here. Similarly, we have

$$\rho = \bar{\rho} + \rho', \quad \mu = \bar{\mu} + \mu'. \tag{9}$$

For turbulent flow with variable density, the density-weighted average, called Favre-average, should be applied to turbulence velocity instead of applying the conventional Reynolds-average, that is

$$U_i = \tilde{U}_i + U_i'', \quad U_i = \overline{\rho U_i} / \bar{\rho}. \tag{10}$$

Then the Favre-average equations for mass and momentum are

$$(\bar{\rho}\tilde{U}_i)_{;i} = 0, \tag{11}$$

$$(\bar{\rho}\tilde{U}_j\tilde{U}_i)_{;j} = -\bar{p}_{;i} +$$
$$+ \left[\bar{\mu}(\tilde{U}_{i;j} + \tilde{U}_{j;i}) - \frac{2}{3}\bar{\mu}\tilde{U}_{l;l}\right]_{;j} - \overline{(\rho U_i'' U_j'')}_{;j} + \bar{f}, \tag{12}$$

where $\tilde{U}_i$ denotes the Favre-average velocity. $\overline{\rho U_i'' U_j''}$ is the Reynolds stress and modeled by the eddy viscosity assumption as

$$\overline{\rho U_i'' U_j''} = -\mu_t\left[(\tilde{U}_{i;j} + \tilde{U}_{j;i}) - \frac{2}{3}\delta_{ij}\tilde{U}_{l;l}\right] + \frac{2}{3}\bar{\rho}K\delta_{ij}.$$

Here δ_{ij} is the Kronecker delta and K is turbulent kinetic energy. In equation (12), the contributions from the viscosity disturbance are neglected and the Favre-average velocity is assumed to be equal to the Reynolds-average velocity, see *Gatski*[10] for details.

The $K - \varepsilon$ turbulence model is applied here and the equations for turbulent kinetic energy and turbulent dissipation rate are

$$(\bar{\rho}\tilde{U}_j K)_{;j} = \left[\left(\bar{\mu} + \frac{\mu_t}{\sigma_k}\right)K_{;j}\right]_{;j} + P - \bar{\rho}\varepsilon, \tag{13}$$

$$(\bar{\rho}\tilde{U}_j\varepsilon)_{;j} = \left[\left(\bar{\mu} + \frac{\mu_t}{\sigma_k}\right)\varepsilon_{;j}\right]_{;j} + c_1\frac{\varepsilon}{K}P - c_2\bar{\rho}\frac{\varepsilon^2}{K}, \quad (14)$$

where μ_t is turbulent viscosity, $P = P_t + P_v$ is the production rate of turbulent kinetic energy, P_t and P_v are corresponding to the turbulent kinetic energy produced by the horizontal turbulent flow and the uprising vapor, respectively. The P_v will be defined in Section 2.1.3. μ_t and P_t are expressed as

$$\mu_t = c_\mu\bar{\rho}\frac{K^2}{\varepsilon}, \quad P_t = -\overline{\rho U_i''U_j''}\,\tilde{U}_{i;j}.$$

The above c_μ, c_1, c_2, σ_k and σ_e are the $K - \varepsilon$ turbulence model constants.

The flow field is shown in Figure 1. The boundary conditions for the equations (11)–(14) are defined below.
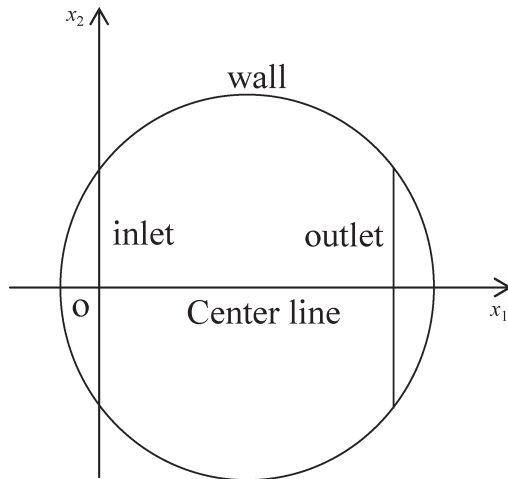

F i g . 1 – *Flow field on the tray*

For the inlet boundary, the inlet liquid velocity distribution is assumed to be uniform. The inlet turbulent kinetic energy and turbulent dissipation rate are described by the following empirical expressions

$$\tilde{U}_{1in} = \frac{L_s}{h_l}, \quad \tilde{U}_{2in} = 0, \quad K_{in} = 0.003\,\tilde{U}_{1in}^2,$$

$$\varepsilon_{in} = \frac{0.09\,K_{in}^{1.5}}{0.03 \times 0.5\,W}. \quad (15)$$

Here, h_l is the clear liquid height.

At the outlet boundary, the flow is assumed being fully developed, then

$$\tilde{U}_{i;1} = K_{;1} = \varepsilon_{;1} = 0. \quad (16)$$

The flow field is symmetric to the centerline. The boundary conditions at the centerline are

$$\tilde{U}_{1;2} = K_{;2} = \varepsilon_{;2} = 0, \quad \tilde{U}_2 = 0. \quad (17)$$

The boundary conditions at tray wall are determined by the wall functions, see *Liu* et al.[4]

We drop all superscripts of averaged quantities in the present and subsequent sections, i.e. write $\tilde{U}_i$ as U_i and $\bar{\rho}$ as ρ for simplification.

Phase volume fraction and clear liquid height

The condition of two-phase flow on trays is in one of the following three different regimes: bubble regime, drop (spray) regime and froth regime. In most cases, column trays are operated in froth regime, see *Stichlmair* and *Fair*[11] for a detailed discussion.

By comparing many published correlations for the volume fraction of liquid phase, *Stichlmair*[12] suggested that the volume fraction of liquid phase can be approximated as

$$\phi_1 = 1 - \left(\frac{F}{F_{max}}\right)^{0.28}, \quad (18)$$

where $F = U_g\sqrt{\rho_2}$ is the vapor load factor and $F_{max} = 2.5[\alpha_p^2\sigma g(\rho_1 - \rho_2)]^{0.25}$ is the maximum vapor load factor. The equation (18) is valid for $F < 3$, and all cases calculated here are in this range.

The height of clear liquid h_l is given by experiments (see *Yu* et al.[3]) as

$$h_l = 8.04 + 3.05\,L_s + 2.523\,h_w^{0.5} - 3.612 \times 10^{-3}F^2. \quad (19)$$

Resisting force exerted by vapor phase

The uprising vapor, which crosses the flowing aerated liquid, or liquid mixture, on a distillation tray, undergoes mutual momentum exchange. Consequently, the uprising vapor exerts a resisting force on the flow and this resisting force is approximated by (see *Zhang* and *Yu*[2])

$$f = -c_f\frac{\rho_2 U_g U_i}{h_l}, \quad (20)$$

where the coefficient c_f reflects the imperfect momentum exchange between the uprising vapor and the flowing aerated liquid on the tray. The above expression implies a hypothetical assumption that the vapor phase leaving the flow surface obtains a horizontal velocity component equal to $c_f U_i$. It is obvious that c_f depends on the height of clear liquid. After many tests, we choose $c_f = 1.7\,h_l$ in all our calculations.

For the convenience of statement, we designate afterward the "aerated liquid" as "liquid phase".

Turbulent energy created by bubbling action

Besides the resisting force exerting on the flow, the uprising vapor offers a direct contribution to the turbulent energy on the liquid phase flow. This fact is obvious because the liquid phase on the tray is fluctuating even if its mean velocity is zero, i.e. no liquid phase flow. The quantity of this extra turbulent energy, P_v, is related to the operating conditions.

For simplification, the uprising vapor through a single hole of sieve plate is considered to estimate the turbulent energy from bubbling action. In principle, such a flow consists of three essential periods, i.e. a converging period before the plate, a diverging period after the plate and finally, the period of passing through the flowing layer, as shown in Figure 2.
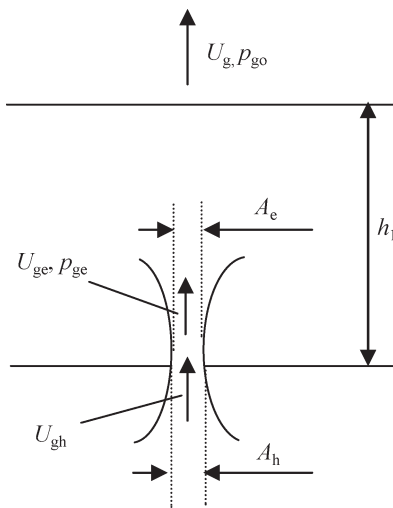

F i g . 2 – *Vapor passing a sieve plate hole*

The velocity U_{ge} is related to the gas velocity U_{gh} by the mass conservation, via

$$U_{ge} = \frac{U_{gh} A_h}{A_e} = \frac{U_{gh}}{a_h} = \frac{U_g}{a_h a_p}, \qquad (21)$$

where the hole discharge coefficient, a_h is 0.611 for the sharp edged holes at high Reynolds number, see *Stichlmar* and *Fair*[11] for details, a_p is the relative free area of the sieve tray.

The pressure loss during vapor passing through the flow layer is approximately determined by considering the pressure loss along a pipe with a nozzle inside, see *Olson* and *Shelstad*,[13] we have

$$p_{ge} - p_{go} = \rho_2 U_g (U_g - U_{ge}). \qquad (22)$$

Then, the pressure head loss for the uprising vapor is

$$\Delta h = \frac{p_{ge} - p_{go}}{g\, p_2} + \frac{U_{ge}^2 - U_g^2}{2g} - h_l =$$

$$= \frac{U_g^2}{2g\, a_h^2 a_p^2} (1 - a_k a_p)^2 - h_l. \qquad (23)$$

Since the pressure head loss h_l is consumed to overcome the hydrostatic pressure head, the vapor energy loss per volume, which produces the turbulent kinetic energy, is expressed as

$$P_v = c_p \frac{\rho_2 (g\Delta h + gh_l)U_g}{h_l} = \frac{c_p \rho_2 U_g^3}{2 a_h^2 a_p^2 h_l}(1 - a_h a_p)^2. \quad (24)$$

Where c_p is a parameter for imperfect energy transfer between the uprising vapor and the flow on a tray. Obviously, it will depend on the inlet velocity and the height of clear liquid. We suggest using the empirical expression

$$c_p = 6.63 \times 10^{-9} U_{in}^2 h_w^3. \qquad (25)$$

Mass transfer model

The successful application of the CFD to the prediction of velocity field on a tray may lead to the development of a method to evaluate the corresponding concentration field, from which the estimation of tray effectiveness can be established on a more theoretical and reliable basis. In this study, we suppose the mass transfer between vapor and liquid phases has no influence on the velocity field on the tray. This assumption is reasonable if the rate of mass transfer between the two phases is not very high. The effect of mass transfer on the velocity field will be a subject of another study.

In distillation process, counter-diffusion occurs simultaneously. That means the light component diffuses from liquid to vapor phase and, at the same time, the heavy component diffuses from vapor to liquid phase. In the present paper, we only concern one plate (tray) where the mass concentration change is usually very small, possibly from few percents to little over ten percents. In a narrow concentration range, the change of heat of vaporization is relatively small and therefore, in engineering practice, we may assume the amount of counter-diffusion to be approximately equal over a plate (tray). For the computation of whole column, it should be considered the change of the heat of vaporization over the whole mass concentration range.

In our model, we consider the composition of vapor phase being identical with that of bubbles or froth. The governing equations for the equal molar transfer in the liquid phase, containing bubbles and froth, are expressed as

$$(\phi_1 U_j C_1)_{;j} - (D_1 \phi_1 C_{1;j})_{;j} + k_1 a(C_1 - C_1^i) = 0, \quad (26)$$

$$(\phi_2 U_j C_2)_{;j} - (D_2 \phi_2 C_{2;j})_{;j} + k_2 a(C_2^i - C_2) = 0, \quad (27)$$

where C_1' and C_2' are the concentrations of light component at the liquid and bubbles (or froth) respectively.

Considering the turbulent effects of the flow field, the following fluctuation equations can be written

$$C_i = \overline{C}_i + C_1', \quad C_i^i = \overline{C}_i^i + C_i^{i'}, \quad (28)$$

$$k_i = \overline{k}_i + k_i', \quad a = \overline{a} + a', \quad (29)$$

Substituting the above equations together with equations (8) and (10) into equations (26) and (27) and neglecting the correlation of any two scalar disturbances and the higher order correlation such as $\overline{\rho' C_i'}, \overline{k_i' a'}, \overline{a C_i'}, \overline{\rho' C_i' U_j''}$ etc., see *Abou-Arab*,[14] as well as replacing the correlation $\overline{U_j'' C_i'}$ by

$$\overline{U_j'' C_i'} = -D_t \overline{C}_{i;j}. \quad (30)$$

then the equations (26) and (27) become

$$(\phi_1 U_j C_1)_{;j} - [(D_1 + D_t)\phi_1 C_{1;j}]_{;j} + \\ + k_1 a(C_1 - C_1^i) = 0, \quad (31)$$

$$(\phi_2 U_j C_2)_{;j} - [(D_2 + D_t)\phi_2 C_{2;j}]_{;j} + \\ + k_2 a(C_2^i - C_2) = 0, \quad (32)$$

where D_t is the phase turbulent diffusion coefficient. As stated in previous section, all superscripts of averaged quantities are dropped, i.e. $\widetilde{U}_i$ written as U_i and $\overline{\rho}$ as ρ for simplification.

Furthermore, by substituting $C_i = \rho \dot{x}_i$ into equations (31) and (32), we have

$$\phi_1 U_j \dot{x}_{1,j} - \phi_1 [(D_1 + D_t)\dot{x}_{1;j}]_{;j} + \\ + k_1 a(\dot{x}_1 - \dot{x}_1^i) = 0, \quad (33)$$

$$\phi_2 U_j \dot{x}_{2,j} - \phi_2 [(D_2 + D_t)\dot{x}_{2;j}]_{;j} + \\ + k_2 a(\dot{x}_2^i - \dot{x}_2) = 0, \quad (34)$$

The mass transfer flux between liquid and gas phases can be expressed as

$$N_s = \dot{k}_1(\dot{x}_1 - \dot{x}_1^i) = k_2(\dot{x}_2^i - \dot{x}_2) = \\ = K_1(\dot{x}_1 - \dot{x}_1^*) = K_2(\dot{x}_2^* - \dot{x}_2). \quad (35)$$

where N_s is the mass transfer flux between the two phases. $\dot{x}_1^i$ and $\dot{x}_2^i$ are the molar concentrations of

light component at the interface and can be approximately expressed by Raoult's law as

$$\dot{x}_1^i = \gamma \, p^0 \dot{x}_2^i = H \dot{x}_2^i. \quad (36)$$

Then from equations (35) and (36), we have

$$K_1 = \frac{k_1 k_2}{H k_1 + k_2}, \quad K_2 = \frac{H k_1 k_2}{H k_1 + k_2},$$

$$\dot{x}_1^* = H \dot{x}_2, \quad \dot{x}_1 = H \dot{x}_2^*. \quad (37)$$

Substituting equations (35) and (37) into equations (33)-(34), we have

$$\phi_1 U_j \dot{x}_{1,j} - \phi_1 [(D_1 + D_t)\dot{x}_{1;j}]_{;j} + \\ + K_1 a(\dot{x}_1 - H\dot{x}_2) = 0, \quad (38)$$

$$\phi_2 U_j \dot{x}_{2,j} - \phi_2 [(D_2 + D_t)\dot{x}_{2;j}]_{;j} + \\ + K_2 a \left(\frac{\dot{x}_1}{H} - \dot{x}_2 \right) = 0. \quad (39)$$

The boundary condition for equations (38) and (39) is described below.

For the inlet boundary, we assume the concentrations of light component in liquid and in carrying bubbles or froth are $\dot{x}_{1in}$ and 0, respectively, i.e.

$$\dot{x}_1 = \dot{x}_{1in}, \quad \dot{x}_2 = 0. \quad (40)$$

At the outlet boundary, the concentration field of light component is assumed being fully developed, then

$$\dot{x}_{i;1} = 0. \quad (41)$$

The mass fraction field is symmetrical to the centerline and the boundary condition is

$$\dot{x}_{i;2} = 0. \quad (42)$$

On the wall, since it cannot be penetrated by the light component, the boundary condition may be written to be

$$\frac{\partial \dot{x}_i}{\partial r} = 0. \quad (43)$$

Mass transfer coefficients and interfacial area

According to *Stichlmar* and *Fair*,[11] the mass transfer coefficients in liquid and vapor sides can be estimated by the following equations, applicable to froth and drop regimes

$$k_1 = \sqrt{\frac{4\phi_1 D_1 U_g}{\pi \, h_l \phi_2}}, \quad k_2 = \sqrt{\frac{4\phi_1 D_2 U_g}{\pi \, h_l \phi_2}}. \quad (44)$$

The interfacial area can be expressed, respectively, for bubble regime as follows ($F/F_{max} > 0.35$)

$$a_b = \left[\frac{6g(\rho_1 - \rho_2)}{\sigma}\right]^{0.5}\left(\frac{F}{F_{max}}\right)^{0.28}. \quad (45)$$

and for drop regime ($F/F_{max} > 0.55$)

$$a_d = \frac{F^2}{2\sigma a_p^2}\left[1 - \left(\frac{F}{F_{max}}\right)^{0.28}\right]. \quad (46)$$

For the interfacial area of froth regime ($0.35 < F/F_{max} > 0.55$), *Stichlmar* and *Fair*[11] suggested to interpolate the interfacial areas of bubble regime and drop regime (equations (45) and (46)). Here we take the weighted average of the interfacial areas of bubble regime and drop regime as that of froth regime,

$$a_f = \frac{(0.55 - F/F_{max})a_b + (F/F_{max} - 0.35)a_d}{(0.55 - 0.35)}. \quad (47)$$

Evaluation of mass transfer efficiency

The mass transfer efficiency of a tray is related to the concentration distribution. For the generalization of concentration expression, a dimensionless liquid concentration X_i is introduced and defined as follows

$$X_i = \frac{\dot{x}_i - \dot{x}_i^*}{\dot{x}_{iin} - \dot{x}_i^*}. \quad (48)$$

In which $X_i = 1$ and $X_i = 0$ represent the initial and equilibrium conditions, respectively.

Substituting $\dot{x}_i^*$ (see equation (37)) into equation (48), the dimensionless liquid concentration becomes

$$X_1 = \frac{\dot{x}_1 - H\dot{x}_2}{\dot{x}_{1in} - H\dot{x}_2}. \quad (49)$$

We now define a new term η, called the relative mass transfer efficiency of a tray or simply the relative tray efficiency, to be the ratio of the average dimensionless liquid concentration on the whole tray to that at the outlet weir. Thus $\eta = 1$ represents the condition of perfect mixing of liquid phase on the tray. In the case of partial mixing of liquid phase, η is greater than 1. Under the condition of no mixing, i.e. the plug flow, η reaches to maximum value. Obviously, η is a measure of the mixing characteristics on a tray, similar to the conventional expression of enhancement factor, E_{MV}/E_{OG}. The value of η can be conveniently computed by the value of X_1 at each grid obtained from the numerical computation as follows

$$\eta = \frac{\frac{1}{n_p}\sum_{i=1}^{n_p} X_{1i}}{\frac{1}{n_w}\sum_{i=1}^{n_w} X_{1i}}. \quad (50)$$

Then the computation of η, the relative tray efficiency of a tray, is possible by the aid of CFD.

Numerical results and discussion

The discretization of the mixed turbulent two-phase flow model (equations (11)–(14)) at grids is performed by finite volume method. The discrete control equations are solved by SIMPLEC algorithm, see *Doormal* and *Raithby*[15] for details. After the velocity field on the tray is obtained, the mass transfer model (equations (38) and (39)) is solved to compute the concentration distribution of light component and the relative tray efficiency η.

The $K - \varepsilon$ turbulence model constants based on the experimental work of *Launder*[16] in a tunnel flow are

$$c_1 = 1.44, \ c_2 = 1.92, \ c_\mu = 0.09, \ \sigma_k = 1.0, \ \sigma_\varepsilon = 1.3.$$

The numerical results of *Yu* et al.[3] show the above constants should be modified in order to fit the experimental data for sieve trays. After a number of trials, the constants $c_1 = 1.48$ and $c_2 = 1.98$ are found to be more sensitive than other constants. For the best fitting, they suggested to use c_1 and c_2 for tray velocity simulation. In the present study, constants $c_1 = 1.48$, $c_2 = 1.98$, $c_\mu = 0.09$, $\sigma_k = 1.0$, $\sigma_\varepsilon = 1.3$. are adopted in all our calculations.

Our numerical simulation is based on two experimental trays. We call the tray, on which *Porter* et al.[17] carried on their experiment, to be Porter tray and the tray, on which *Liu*[18] did his experiment, to be Liu tray. The geometric parameters for Porter tray and Liu tray are $D = 2.44$ m, $W/D = 0.615$ and $D = 1.2$ m, $W/D = 0.645$, respectively. In this study, $\rho_1 = 1000$ kg m^{-3}, $\mu_1 = 1 \times 10^{-3}$ kg m^{-1} s^{-1}, $\rho_2 = 1.2$ kg m^{-3} and $\mu_2 = 2 \times 10^{-5}$ kg m^{-1} s^{-1} are adopted as the density and viscosity of the two phases, respectively.

According to the rule of similarity, there exists a relationship between the turbulent kinematic viscosity and the turbulent diffusion coefficient. *Yu* et al.[3] show that slightly different ratio of the above two parameters does not change substantially the results of the concentration profile on the tray. Here we take their suggested relationship $D_t = 1.25 \mu_t/\rho$ for all calculations.

Flow field simulation

Figures 3 shows the comparison of the results of our mixed two-phase flow model with those by experiments. Here the percentage of circulation region T is defined as the ratio of the circulation area to the whole tray area. This parameter is essentially important for sieve tray design. In fact, the T value should be reduced to be as small as possible to achieve the best velocity distribution and the relative tray efficiency.
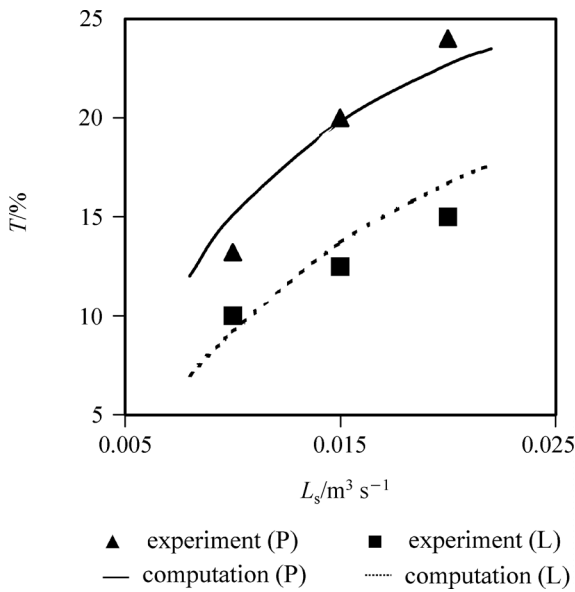
T a b l e 1 – *The addopted parameters of diferent computing cases*

Unit	L_s m² s⁻¹	h_w mm	U_g m s⁻¹	α_p	σ N m⁻¹	H	D_1 m² s⁻¹	D_2 m² s⁻¹
Figure 4	0.02	20	1.5	0.1	0.1	2	10^{-9}	10^{-6}
Figure 5		20	1.5	0.1	0.1	2	10^{-9}	10^{-6}
Figure 6	0.02		1.5	0.1	0.1	2	10^{-9}	10^{-6}
Figure 7	0.02	20		0.1	0.1	2	10^{-9}	10^{-6}
Figure 8	0.02	20	1.5		0.1	2	10^{-9}	10^{-6}
Figure 9	0.02	20	1.5	0.1		2	10^{-9}	10^{-6}
Figure 10	0.02	20	1.5	0.1	0.1		10^{-9}	10^{-6}

▲ experiment (P)　　■ experiment (L)
— computation (P)　　‥‥‥ computation (L)

F i g . 3 – *The percentage of circulation region % vs. liquid flow rate. Porter tray (P): D = 2.44 m, h_w = 20 mm, U_g = 1.5 ms⁻¹, Liu tray (L): D = 1.20 m, h_w = 50 mm, U_g = 1.0 ms⁻¹*

It is found that the T value increases with the increase of input liquid flow rate L_s and the results of our numerical flow model are in a good agreement with the corresponding experiments.

Relative tray efficiency η estimation

Table 1 shows the adopted parameters of Figures 4–10. Figure 4 is the contour map of dimensionless concentration in liquid X_1 on sieve tray. It shows there is a large backward mixing area (vortex) near the tray wall and the X_1 value is low at that area. Then the relative tray efficiency η is greatly reduced by the backward mixing effects. The larger the mixing area, the smaller the plate effectiveness is.

Figure 5 shows the dependence of η on the input liquid flow rate for Porter tray and Liu tray. For both trays, the η value decreases with the increase of L_s. The reason is that with the increase of L_s the input liquid velocity is increased and results in the increase of the percentage of circulation region. It is noted that the η value of Porter tray is always larger that of Liu tray as seen from Figures 5–10.
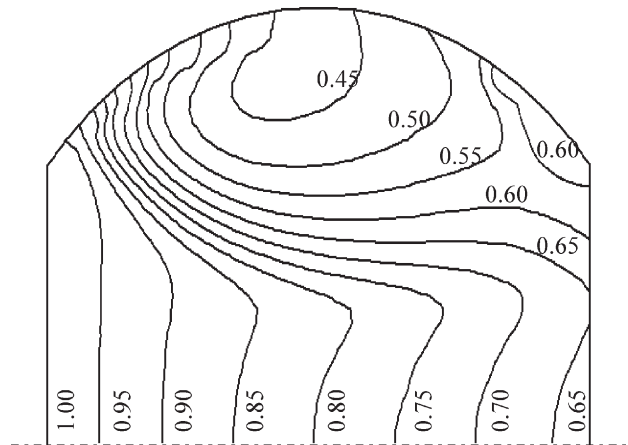

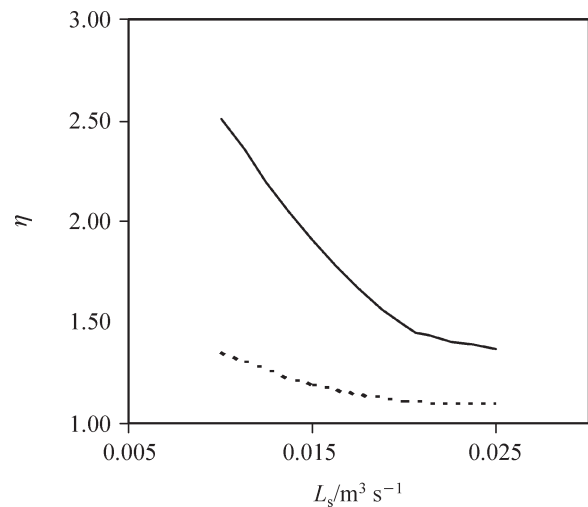F i g . 4 – *Contour map of liquid dimensionless concentration on Liu Tray*

F i g . 5 – *Relative tray efficiency vs. liquid flow rate. Solid line: Porter tray, dashed line: Liu tray*

Figure 6 shows the dependence of η on the height of outlet weir h_w. As h_w increases, the input liquid velocity is decreased for the same input liquid flow rate. Based on the same explanation for Figure 5, the η value is increased with the increase of h_w. But this dependence on h_w is much weaker than that on L_s.

Figure 7 shows that the η value increases with the increase of superficial gas velocity for both trays. With the increase of U_g, the mass transfer coefficients k_i and the turbulent kinetic energy P_v produced by the uprising vapor are increased. The increase of P_v will results in the reduction of the backward mixing area. Both reducing the mixing area and increasing the mass transfer coefficients can increase the η value.

Figure 8 shows the dependence of η on α_p. The value of η decreases fast with the increase of α_p when $\alpha_p < 0.1$ for Porter tray and $\alpha_p < 0.08$ for Liu

tray. Then the decrease changes to be slight. The reason for this change may be explained as follows. With the increase of α_p, P_v and α_d decrease and causes the lowering of η. On the other hand, ϕ_1 increases with the increase of α_p. This leads to the increase of k_1 and k_2 and cause the increase of η. These two opposite effects cause the η value decreases slightly with the increase of α_p.

Figure 9 shows the dependence of η on σ. The value of η decreases fast with the increase of σ when $\sigma < 0.05$ for both trays. Then it decreases slightly when $\sigma > 0.05$. The effects of σ on the value η are very complex and have at least three aspects. Firstly, the interfacial area is decreased with the increase of σ and this effect causes the decrease of η. Secondly, ϕ_1 increases with the increase of σ, which leads to the increase of k_1 and k_2 and cause the increase of η. Thirdly, the increase of σ also changes the mixture of vapor and liquid, which may
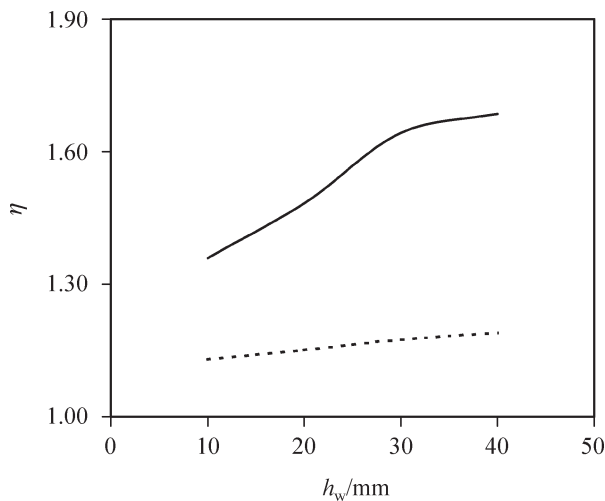

Fig. 6 – *Relative tray efficiency vs. outlet weir height. Solid line: Porter tray, dashed line: Liu tray*
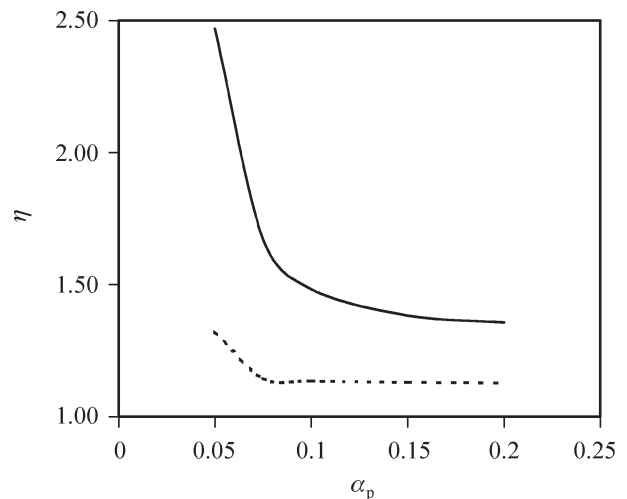

Fig. 8 – *Relative tray efficiency vs. plate free area rate. Solid line: Porter tray, dashed line: Liu tray 2*
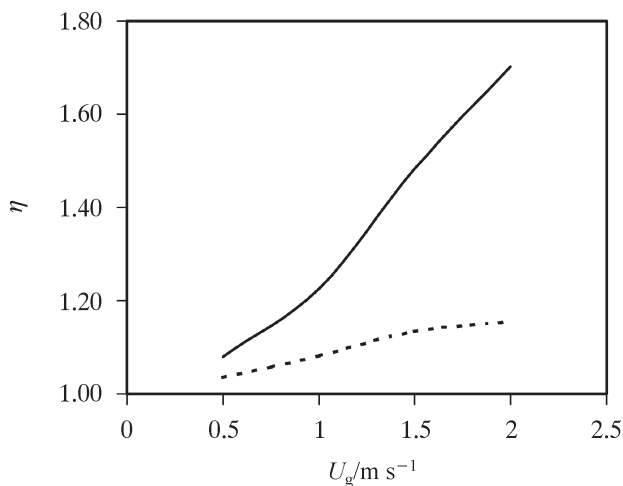

Fig. 7 – *Relative tray efficiency vs. superficial gas velocity. Solid line: Porter tray, dashed line: Liu tray*
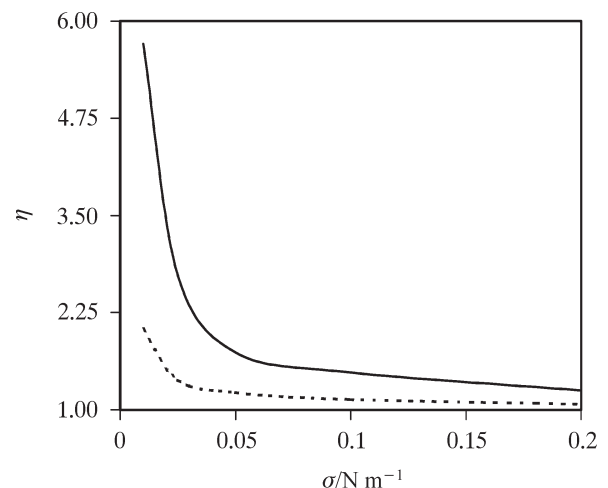

Fig. 9 – *Relative tray efficiency vs. surface tension. Solid line: Porter tray, dashed line: Liu tray*

change the Reynolds number and turbulence intensity of the flow field, and results in the change of velocity field and the η value. The first two effects are local effects that are independent on tray diameter, but the third effect is an effect on the whole tray (flow field), which surely depends on the tray diameter.

Figure 10 shows the dependence of η on H. The results indicate that η increases slightly with the increase of H. The constant H shows the interfacial resistance when mass transferring at the interface. The higher value of H means the smaller drive force term of interfacial mass transfer $K_1(\dot{x}_1 - H\dot{x}_2)$ in equations (38) and (39) if the two-film model is adopted. For the flow field of the same tray, this is similar to the case of the two phases with less on-tray contact time, such as the plug flow case, where η gets to a larger value. Here we should note that the constant H we put in Raoult's law is only valid for small concentration range of light component in liquid and vapor over a tray. In case of large concentration range of light component, the constant H is varying due to the change of activity coefficient γ with concentration for non-ideal separating system. Fortunately, it is shown that H has only small effects on η. Thus, it is quite safe to say that the deviation introduced by assuming H to be a constant should be negligible.
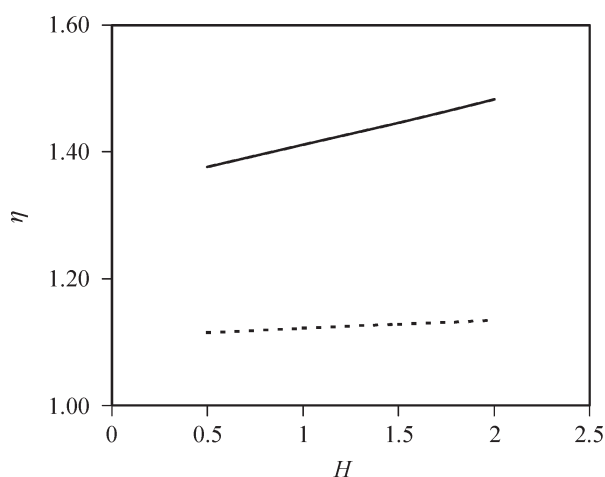

F i g . 1 0 – *Relative tray efficiency vs. H. Solid line: Porter tray, dashed line: Liu tray.*

Our results also show η value increases fast with the increase of D_1. The coefficients of mass transfer K_1 and K_2 increase when D_1 increases and leads to the fast increase of η. On the other hand, the dependence of η on D_2 is very weak and η value increases slightly with the increase of D_2. It is concluded that D_1 has stronger influence on the mass transfer between the liquid and vapor than D_2. This conclusion also comes simply by looking at the

constants of D_1 and D_2. Except the effect of H, the mass transfer of interface is always controlled by the smaller molecular diffusion phase until a equilibrium state is reached.

Conclusions

It is shown, that the turbulent mixed two-phase flow model presented here can be applied to simulate the gas-liquid flow on the tray instead of using the much more complicated two-fluid model without losing much accuracy. Computations show that the percentage of circulation region on the tray has large effects on the relative tray efficiency, i.e. the performance of mass transfer over a tray. The larger the percentage of circulation region is, the smaller the relative tray efficiency. In order to increase the relative tray efficiency, it is necessary to investigate how to reduce the percentage of circulation region.

Numerical results show that the relative tray efficiency can be efficiently increased as a result of improving the flow pattern on a tray. The high relative tray efficiency can be realized by optimized operational and geometric parameters, such as by increasing outlet weir height h_w, superficial gas velocity U_g, or by reducing liquid flow rate L_s and plate free area rate α_p ($a_p < 0.1$).

On the other hand, the relative tray efficiency can also be improved by changing some physical properties of liquid and vapor, such as reducing the surface tension σ in the range of $\sigma < 0.05$. But the constant H, gas diffusion coefficient D_2 and surface tension σ at $\sigma > 0.05$ have only small effects on the relative tray efficiency.

Results also show that the relative tray efficiency of Porter tray (larger diameter tray) responses more strongly to the above discussed ways of improving tray performance than that of Liu tray (smaller diameter tray). This means the mass transfer performance of a large diameter tray is more sensitive to the parameters studied here. This may be explained as: for most of ways above to improve the performance of trays, the flow pattern on the trays always be affected in a way or another. Comparing to a large diameter tray, the inertia of reducing circulation region on a small diameter tray is large due to its large curvature of tray boundary, numerical results show that the circulation of flow affects the relative tray efficiency strongly. That is why the mass transfer performance of a small diameter tray is less sensitive to the parameters studied here.

The distillation process is a very complex system. It is strongly affected by many operational, physical and geometric parameters. To achieve high relative tray efficiency, more study is necessary to

look for the optimal design and operating parameters of a distillation process.

Finally, it should be mentioned that the above ways to improve the mass transfer performance of trays only present a general rule for optimizing or designing trays. Which methods are accepted in a real case is dependent on the carefully consideration and the evolution of all-important factors (including economy and manufacture). It should be avoided, that the improvement of one side by neglecting the price to be paid for this, on the other side.

Notation

a – interfacial area per unit volume

A – area

c_1, c_2, c_μ – $K - \varepsilon$ model constants

c_f – momentum transfer parameter

c_p – energy transfer parameter

c_q – mass transfer parameter

C – concentration of light component

D – tray diameter

D_i – phase molecular diffusion

D_t – phase turbulent diffusion

E – interfacial friction coefficient

E_{MV} – Murphree tray effectiveness

E_{OG} – Murphree point effectiveness

f – body and external force.

F – vapor load factor

g – acceleration due to gravity

H – constant put in Raoult's law

h_l – clear liquid height

h_w – outlet weir height

K – turbulent kinetic energy

K_i – mass transfer coefficient

k_i – phase mass transfer coefficient

L_s – liquid flow rate

N_s – mass transfer flux between phases

n_p – grid number on tray

n_w – grid number at outlet weir

p – pressure

p^0 – saturation vapor pressure

P – turbulent energy production

P_v – turbulent energy produced by uprising vapor

R – tray radius

r – radial coordinate

T – percent of circulation region

U_g – superficial gas velocity

U_i, V_i – phase velocity

W – width of outlet weir

x_i – Cartesian coordinates

$\dot{x}_i$ – molar concentration of light component

$\dot{x}_i^*$ – equilibrium molar concentration

X_i – phase dimensionless concentration

Greek symbols

α_h – area rate

α_p – free area rate of sieve tray

ε – turbulent energy dissipation rate

η – relative tray efficiency

μ – mixture viscosity

μ_i – phase viscosity

μ_t – turbulent viscosity

ρ – mixture density

ρ_i – phase density

σ – surface tension

σ_k, σ_ε – $K - \varepsilon$ model constants

ϕ_i – phase volume fraction

Superscripts

$-$ – Reynolds-average value

$'$ – disturbance in Reynolds-average

$\sim$ – Favre-average value

$"$ – disturbance in Favre-average

i   – phase interfacial surface

Subscripts

1   – liquid phase or light component in liquid phase

2   – vapor phase or light component in vapor phase

;i   – derivative with respect to x_i

b   – bubble

d   – drop

f   – froth

h   – hole

in   – value at inlet weir

References

1. *Yoshida, H.,* Chem. Eng. Comm. **51** (1987) 261.
2. *Zhang, M. Q., Yu, K. T.,* Chinese J. Chem. Eng. **2** (1994) 63.
3. *Yu, K. T., Liu, C. J., Yuan, X. G..,* 1999 Annual Meeting of American Institute of Chemical Engineers, Dallas.

4. *Liu, C. J., Yuan, X. G., Yu, K. T.,* Chem. Eng. Sci. **55** (2000) 2287.

5. *Yuan, X. G., You, X. Y., Yu, K. T.,* J. Chem. Ind. Eng. (China) **46** (1995) 511.

6. *Yu, K. T., Yuan, X. G., You, X. Y., Liu, C. J.,* Chem. Eng. Res. Des. **77** (1999) 554.

7. *Krishna, R., van Baten, J. M., Ellenberger, J., Higler, A. P., Taylor, R.,* Chem. Eng. Res. Des., **77** (1999) 639.

8. *van Baten, J. M., Krishna, R.,* Chem. Eng. J. **77** (2000) 143.

9. *Elghobashi, S. E., Abou-Arab, T. W.,* Phys. Fluids **26** (1983) 931.

10. *Gatski, T. B.,* Turbulent flows: model equations and solution methodology, Computational Fluid Mechanics, ed. Peyret, R., Academic press, 1996.

11. *Stichlmair, J. G., Fair, J. R.,* Distillation, Wiley-VCH, 1998.

12. *Stichlmair, J. G.,* Grundlagen der Dimensionierung des Gas/Fluessigkeit-Kontakt-apparates Bodenkolonnen Verlag Chemie, Weinheim, New York, 1978.

13. *Olson, S. T., Shelstad, K. A.,* Introduction to fluid flow and the transfer of heat and mass, Prentice-Hall, Inc., 1987.

14. *Abou-Arab,* T. W., Turbulence model for two-phase flows, Encyclopedia of Fluid Mechanics, Vol. 3, Ed. Cheremisinoff, N. P., Gulf Publishing Company, 1985.

15. *van Doormal, J., Raithby, G. D.,* Numer. Heat Transfer **7** (1984) 147.

16. *Launder, B. E., Morse, A., Rodi, W., Spalding, D. B.,* Proc. of NASA conference on free shear flow, Langley, 1972.

17. *Porter, K. E., Yu, K. T., Chambers, S., Zhang, M. Q.,* Flow patterns and temperature profiles on a 2.44m diameter sieve tray. IChE Symp. Ser., 1992, pp. 128.

18. *Liu, C. J.*, Ph. D. Dissertation, Tianjin university, 1998.